JOURNAL OF
ENVIRONMENTAL HYDROLOGY
The Electronic Journal of the International Association for Environmental Hydrology
On the World Wide Web at http://www.hydroweb.com
VOLUME 13 2005

A HYDROCHEMICAL AND ISOTOPIC STUDY OF SUBMARINE FRESH WATER ALONG THE COAST IN LEBANON

Zeinab Saad[1,2]
Véronique Kazpard[1,2]
Kamal Slim[1]
Moustafa Mroueh[1]

[1]Lebanese University, Faculty of Sciences
[2]Lebanese Atomic Energy Commission
Beirut, Lebanon

The karstic aquifer system and the submarine springs on the Lebanese coast have been studied using chemical and isotopic methods to determine the sources for coastal and submarine springs. Chemical analysis shows that most submarine springs are derived from a Cenomanian-Turonian aquifer with a large influence of the bedrock type including calcite and dolomite. Different physical and chemical characteristics are obtained for some submarine samples located on the southern coast that show high sulfate content. Isotopic data for $\delta^{18}O/\delta^{12}H$ shows that coastal freshwaters are closer to the Mediterranean Meteoric Water Line than the submarine springs. Submarine samples located in the south were located below the Global Meteoric Water Line, indicating differences from the coastal freshwater sources. The calculated percentage of freshwater in the submarine samples ranges from 10 to 96%, with the highest percentage for a spring in the Chekka region. Tritium values of submarine samples (ranging from 0.75 to 3.77 TU) are found to be comparable to the coastal freshwater samples (0.69 to 4.83 TU). Spring waters are divided into two distinct sources: young meteoric water supplies coastal freshwater and the submarine sample in the Chekka region, and older water supplies the submarine springs.

INTRODUCTION

The hydrogeology of Lebanon and the distribution of springs, their location and flow regime, is to a very large extent controlled by the geological structure imposed during the main rifting period. In this respect, Lebanon is notable for the density of its shearing and fracture network, which has the effect of partitioning wide areas of the aquifer, and producing many simple overflow springs throughout the country. Some extend offshore such as one located 3 km offshore of the Litani River mouth (FAO, 1972). Lebanon's hydrogeology is determined by the distribution of the limestones and dolomites and their karstic features (Walley, 1998; Dubertret, 1975). The karstic province covers about 6000 km^2, or about 60 percent of the country, creating subterranean rivers and spring seepage on the lower mountain flanks. Different types of springs can be identified according to their aquifer sources: unconfined (related to Cenomanian and Jurassic aquifers), confined, and semi-confined aquifers (related to karstic aquifers) (Guerre, 1969; Mijatovic et al., 1967).

Submarine springs flow over stratigraphic contacts like transverse fractures superimposed on fold structures. For example, the submarine springs of the Chekka region are estimated to flow at 10 m^3/sec from the Turonian-Cenomanian limestone at a depth of 120 m below mean sea level. The water moves to the sea via a complex of fault and karstic zones and, like other springs, the Chekka springs show a seasonal variation with the strongest flow being recorded in the late winter and early spring period (Qareh, 1966; Hakim, 1985).

Marine springs are well developed in the maritime region along the eastern Mediterranean Sea as in the coastal areas of Lebanon. Complex hydrogeologic conditions create submarine springs as discharge points from coastal aquifers (Hakim, 1985, 1976). Morphology is more dominant in western Lebanon, as shown by channeling systems, (i.e. faults), karstic conduits and paleochannels. Lithology consists of the rocks distributed at the coast (Beydoun, 1977; Dubertret, 1966). The complex hydrogeologic regime results in the formation of submarine springs and seawater intrusion into the coastal aquifers.

The submarine springs can be divided into two groups according to their aquifer sources:

· The Cenomanian-Turonian aquifer, where water from rain and snowmelt percolates through fissured limestone, and then emerges at the coast wherever marls exist as a barrier.

· The Jurassic aquifer, where water percolates into deep beds and appears where faults transect the sea. (Gruvel, 1931).

Studies of submarine water date back to Gruvel (1931), who reported on the distribution of major discharging submarine springs. Other important studies include those reported by Qareh (1966) on the Chekka springs, which included quantitative and hydraulic estimates of discharge of about 10-15 m^3/sec. A more detailed study was conducted by Guerre (1969) to classify the aquifer of sources as unconfined (Cenomanian and Jurassic aquifers) and semi-confined aquifers (karstic aquifers such as those in Chekka).

FAO conducted an airborne thermal infrared survey along the coast of Lebanon in 1972 (FAO, 1972). The major goal was to calculate the discharges of submarine springs for at least 7 km offshore. The infrared radiometer revealed 61 fresh water sources, 15 of them were offshore springs with an average yield of 150-200 l/sec. In 1976, Hakim completed a detailed study on the submarine springs along the coast (Hakim, 1996). He classified the thermal anomalies into several types related to false sources, pollution, river discharge, and offshore springs. The latest studies in this field were

conducted in 1997 by the NCRS using thermal infra-red remote sensing on the northern and southern coast. About 54 submarine springs are identified throughout the offshore zone from the north to the south (NCRS, 2002 in private communication). It was found that 52 % of these springs are from karstic rock formations with high flow rate, 22 % are from fault alignments with high flow rates, and 18 % are offshore springs with low to high flow rates (intemittent flow). The volume of the flow was estimated at about one billion m^3/year (Khawlie et al., 2000). In the south, the presence of hydraulic features was more developed. The features include longer lineament extents, dense fracturing systems and conduit extension to the sea. Twenty-seven thermal anomalies were related to fresh water in the north sector. The southern region has submarine sources discharging similar quantities as the north. Also, a study was conducted to identify the landward hydrologic system of these springs (Shaban, 2001).

These studies do not give precise information about the quality, the origin and the residence time of water that discharges to submarine springs. Also, there is no information about the relation between the aquifers and the hydrochemical quality of water. In this study of the submarine springs, we combined physical and chemical analysis with isotopic techniques as a less costly technique compared to infra red remote sensing. The study goals include the physical and chemical characteristics for water type (originating aquifers) and water quality (chemical parameters), origin of recharge for the submarine springs, residence time in the aquifers, and the amount of mixing between freshwater and seawater.

Materials and methods

A submersible pump with a capacity of 1 l/sec for 100 m depth was constructed locally and was used by divers for sample collection . The pump is constructed in such a way as to sample the water horizontally from the mid point of the discharging flow. The process uses the difference in density of the salt water to isolate the fresh water inside a cone shaped collector placed over the source orifice. To avoid contamination we used a casing twice the diameter of the pump. The discharge water arrives totally through the fabricated device under pressure. A pump is connected to a flexible plastic tube that is equipped with a non-return pressure valve (a check valve). The plastic tube is connected to the sampling bottle on the boat. The sampling arrangement is shown in Figure 1.

A combined hydrochemical and environmental isotope survey was conducted for 22 major freshwater coastal springs (including 10 deep wells) and 10 seawater springs. Sampling points were selected to reflect seasonal variations. Their spatial distribution was as follows (Figure 2): eleven sampling points from the northern part of the coast distributed as S1 to S11, eleven sampling points from the southern part of the coast distributed as S12 to S23, and ten submarine water samples along the Mediterranean coast distributed as M1 to M10.

General descriptions of hydro chemical parameters for all samples are presented in Table 1 (submarine springs) and Table 2 (coastal freshwater). All samples were treated before analyses. Aliquots of water were stored in polyethylene bottles. The rest of the samples were passed through 0.45µm Millipore filters and than refrigerated for analysis. The pH, electrical conductivity (EC), total dissolved solids (TDS) and temperature of the water samples were measured during the sampling in the field. The chemical analyses of the water samples were conducted immediately after their collection. Anions and cations were analyzed with atomic absorption spectroscopy (Perkin Elmer AA 100) and an ion chromatograph (Dionex IC 25). Each sample was analyzed for $\delta^{18}O$, $\delta^{2}H$ and ^{3}H in the Isotope Laboratories of Amman (Jordan) and Damascus (Syrian Atomic Energy Commission).

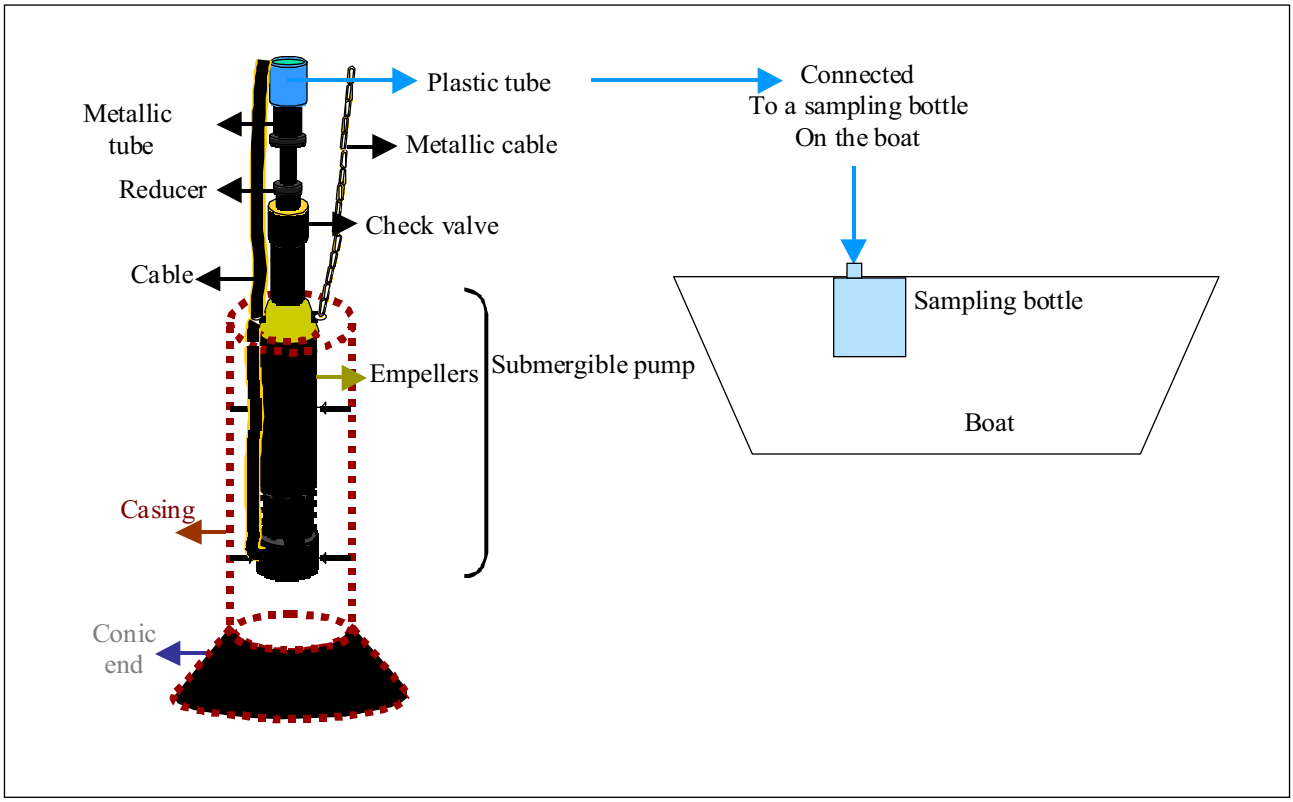

Figure 1. Illustration of sampling procedure.

RESULTS AND DISCUSSION

The most abundant solutes in all coastal waters are Ca, Cl and bicarbonate while Mg and SO_4 are also prominent. For submarine water, Na, Cl and Ca are predominant, while HCO_3 is present in all samples. This chemical composition suggests several water types (Vengosh et al., 2002). The different proportions of the mentioned dissolved ions are used to determine 2 basic water types for submarine waterand 3 basic water types for coastal water .

Facies for submarine water were:

1) Ca-Na-HCO_3-Cl in M2, M3, M4, M6;

2) Ca-Mg-HCO_3-Cl in M5, M9, M10.

These facies reflect the influence of marine water composition regardless of Na and Cl, and the runoff of aquifers with respect to calcite and dolomite nature.

Facies for coastal sources were:

1) Ca-Mg-Cl in S1, S2, S8, S9, S10, S14, S22;

2) Ca-Mg-SO_4-Cl-HCO_3 in S3, S11, S23;

3) Ca-Mg-Cl-HCO_3 in S4, S6, S21.

These sources were derived from a Cenomanian-Turonian aquifer with a large influence of calcite and dolomite bedrock. These types of water are shown in the following piper diagram (Figure 3).

Chemical composition of water samples

Results of chemical analyses of waters are presented in Figures 4 to 7. Total dissolved solids TDS

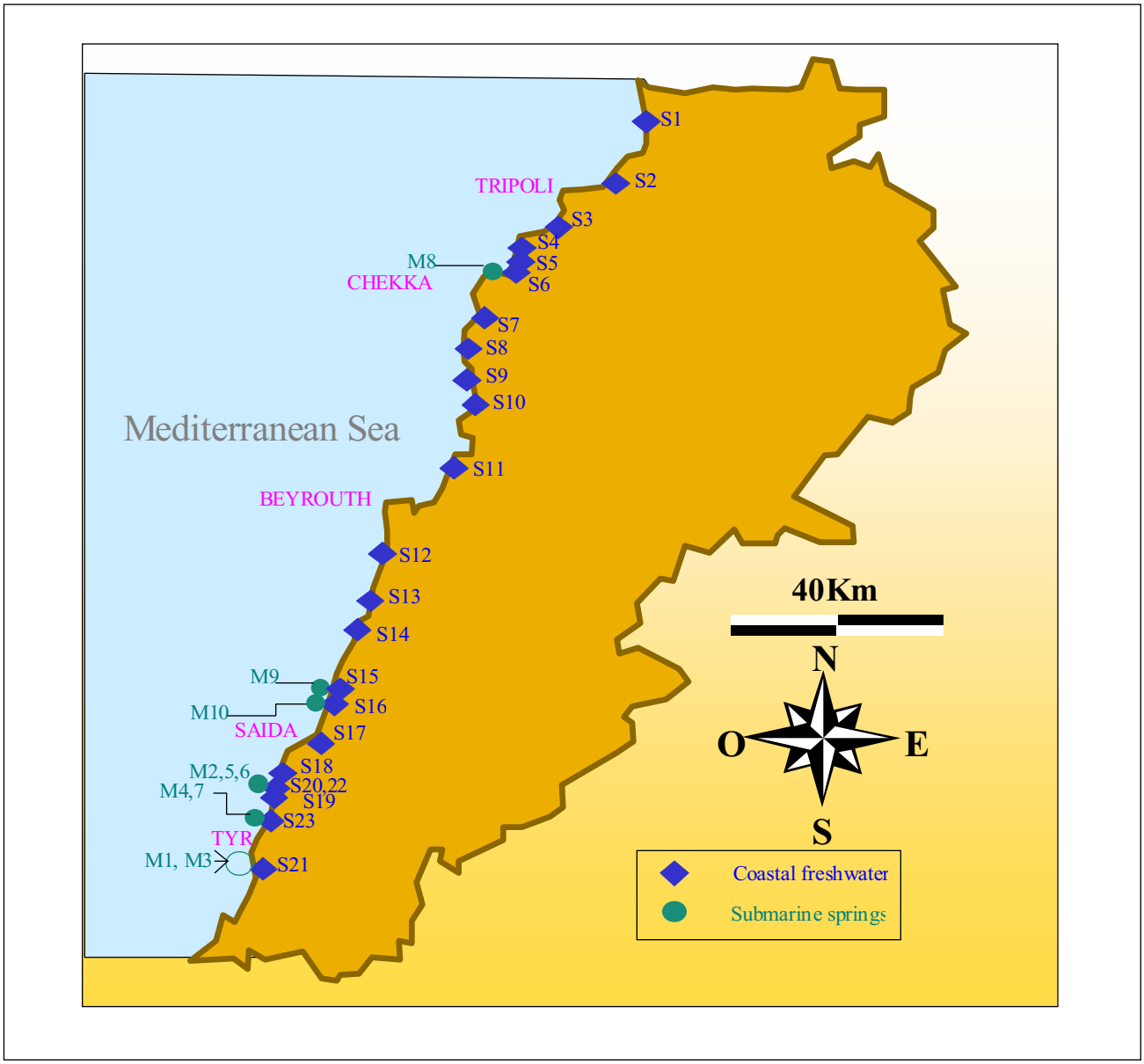

Figure 2. Location of sampling sites along the coast for coastal freshwater and submarine springs.

(Figure 4) for coastal freshwater ranges from 330 to 5700 mg/L (S1 – S23); TDS for submarine water ranges from 7000 to 36000 mg/L (M1 – M10). pH values are near neutral in almost all samples except in M9, M10, S2 and S11 (pH around 8).

Figure 4 also shows the variation of the sum of cations as a function of the sum of anions for all data (submarine and coastal sources). The values are reported in meq/L and the correlation is very high ($r^2 = 0.99$). This indicates that the ions have the same origin and they are in a similar appropriate dissolved form in water.

We report the salinity vs. chloride for submarine water. A very high correlation between these two parameters ($r^2 = 0.9$) indicates that the salinity in these samples (M1-M10) is due to the chloride content. In comparison with seawater (SW on the graph), submarine samples show lower salinity and chloride content. This confirms that our sampling point sources derive essentially from freshwater sources. Inherent in any study of submarine groundwater discharge is the difficulty of isolating true spring or seep water from ambient seawater. Most submarine groundwater discharge occurs as

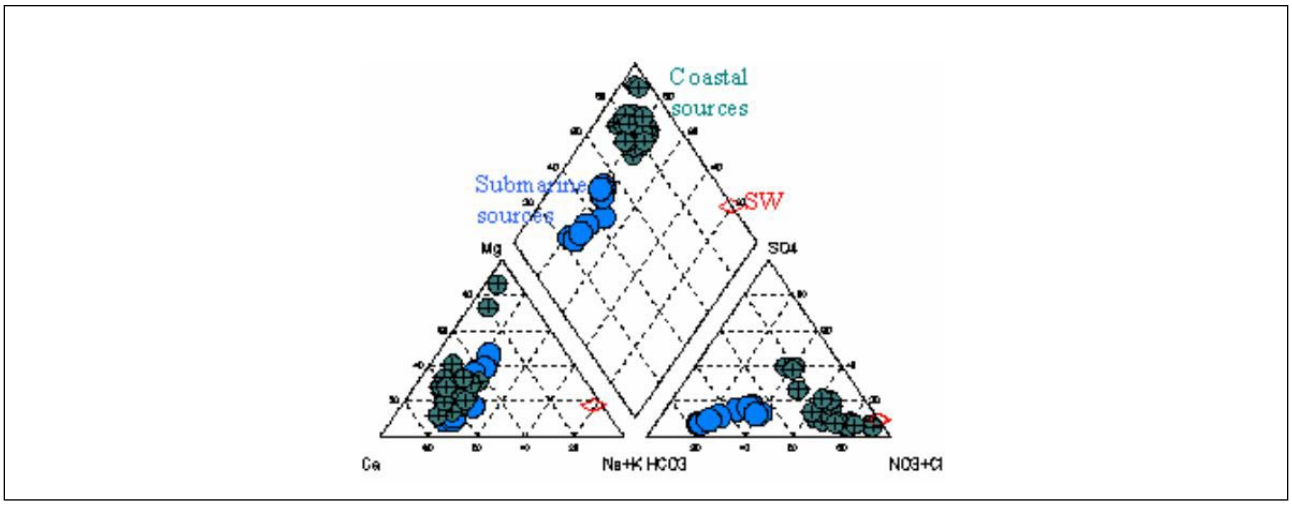

Figure 3. Chemical quality of submarine and coastal sites according to piper diagram.

Table 1. Characteristics of Submarine Spring Sites

Name of station	Coordinates	Corresponding Submarine springs	EC mS/cm	Estimated yield (l/sec)	Main flow featuring	Depth under sea water
Boroghlieh	N33°19'33.7'' E35°10'6.76''	M1	18.3	200	Artesian flow 50 m offshore, 80 m diameter water cone	38m
Adloun-Nsarieh	N33°10'10.1'' E35°10'0.23''	M2	39	500	Irregular huge flow, 500*900m	10m
Boroghlieh	N33°20'7.92'' E35°10'46.7''	M3	19.1	2000	Artesian flow 3000m offshore, 500 m diameter water cone	50m
Abou Al-Aswad	N33°22'19'' E35°15'03''	M4	23.7	100	Chaotic flow	280m
Adloun	N33°23'30'' E35°15'19''	M5	55.9 (T>40° C)	200	Chaotic seepage, 80m in diameter	30m
Adloun	N33°23'30'' E35°15'19''	M6	56.4 (T>40° C)	200	Chaotic flow, 80 m in diameter	30m
Abou Al-Aswad	N33°22'19'' E35°15'03''	M7	21.4	100	Chaotic flow	280m
Chekka	N34°20'22.4'' E35°43'25.3''	M8	13.4	6000	Apparent surface water leaking from beach and parallel to it, spreading 10 – 15 m; 700 m offshore, 60 m diameter	19m
West Saida	N33°35'7.7'' E35°22'44.1''	M9	57.8 (T>40° C)	175	Linear flow into offshore, 500 m	13m
East Saida	N33°34'9.59'' E35°22'55''	M10	57.1 (T>40° C)	175	Linear flow into offshore, 400 m	13m

Table 2. Characteristics Coastal Freshwater Springs along the Lebanese Coast from North to South

Name of station	Coordinates	Coastal Sources	EC (mS/cm)	Altitude over sea water
Aboudiyeh	N34°38'3.22'' E36°00'07''	S1	10.6	16m
Minieh	N34°27'46.6'' E35°56'22.7''	S2	0.8	100m
Abou-halaa	----	S3	0.8	Sea level
Nabeh el Gear	N34°21'4.1'' E35°44'4.2''	S4	1.1	17m
Abar Jradi	N34°20'3'' E35°44'13.7''	S5	0.58	41m
Chekka	N34°16'5.4'' E35°39'38.1''	S6	1.27	20m
Al Helwe	N34°14'45.2'' E35°39'38.6''	S7	1.1	17m
Halat	N34°5'11.1'' E35°39'3.1''	S8	1.9	15m
Bwarr	N34°2'40.8'' E35°37'51.1''	S9	1.5	2m
Nabeh Taffaha	N34°5'5.3'' E35°28'57.4''	S10	5.6	27m
Nahr El founoun	N33°57'17.2'' E35°36'6.4''	S11	0.6	7m
Khalde	N33°42'41.6'' E35°27'5.1''	S12	6.8	10m
saadiyatt	N33°41'5.7'' E35°25'20.7''	S14	2.3	28m
West Saida	N33°37'14.5'' E35°24'17.8''	S15	2.3	15m
East Saida	N33°36'44.20'' E35°24'12''	S16	2.11	24m
El Brak	N33°28'59.1'' E35°19'28''	S17	0.77	16m
Khayzarann	----	S18	0.96	Sea level
Sakssakiyyeh	N33°26'17.9'' E35°17'24.5''	S19	0.9	150m
Adloun	N33°22'0.2'' E35°16'4.4''	S20	1.9	53m
Boroghlieh	N33°18'15.15'' E35°14'31.4''	S21	2	80m
Adloun-Nsarieh	N33°22'0.2'' E35°16'4.4''	S22	1.17	53m
Abou Al-Aswad	N33°22'10.1'' E35°16'55.7''	S23	0.62	47m

diffuse seepage, and identifying sites of submarine groundwater discharge or quantifying flux rates of this discharge across the sediment-water interface is difficult.

Spatial variation of some chemical parameters

Figure 5 shows the spatial variation along the coast of major cations and anions in water. The chemical composition of submarine water (M1-M10) shows higher ion concentrations for almost all elements than the coastal sources (S1-S23). Ca and HCO_3 concentration shows the same variation trend from S1 to S23 and from M1 to M10. Also higher concentrations for Cl-SO_4 and Mg-K are shown in submarine sampling stations. For all these elements, we observe a decrease in the concentration in Stations M7 and M8. This decrease indicates that additional processes and/or solute sources are involved in generating the solute composition.

Chlorine results

Figure 6 shows selected Cl variation diagrams in comparison to the Mediterranean seawater (SW)

concentration. Such plots can help evaluate the origin of water solutes. If samples plot near the seawater composition, their solutes may represent simple dilution of seawater or the dissolution of marine aerosols in the recharge area along the coast. Deviations from the SW composition indicate potential solute sources contributing to the chemistry of water such as subsurface reaction with regional sedimentary rocks including the aquifer materials (Struchio et al., 1996).

In the Na vs. Cl graph, samples are divided between those simply diluted with seawater and those enriched in Na due to the dissolution of Na minerals.

Figure 6 also shows that almost all waters are enriched in Ca and Mg relative to SW. This implies that dissolution of Ca and Mg minerals such as calcite and dolomite has occurred. Possible sources of these elements are the Upper Cretaceous and Eocene carbonate rocks that are found throughout much of the region. The enrichment in Mg may indicate that some of the excess of Ca was derived from the dissolution of dolomite. Mg-Cl and K-Cl diagrams show two distinct water types for submarine springs separated from coastal springs. The distinct group within the submarine springs, corresponds to samples M5, M6, M9, M10. In the following study, we will try to identify the nature of this group.

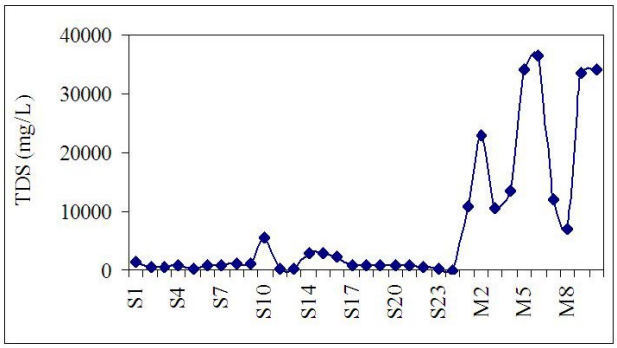

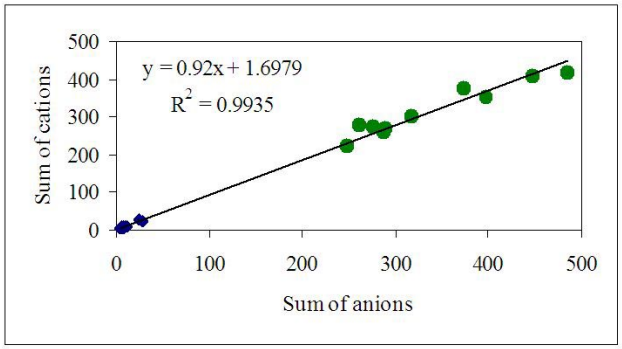

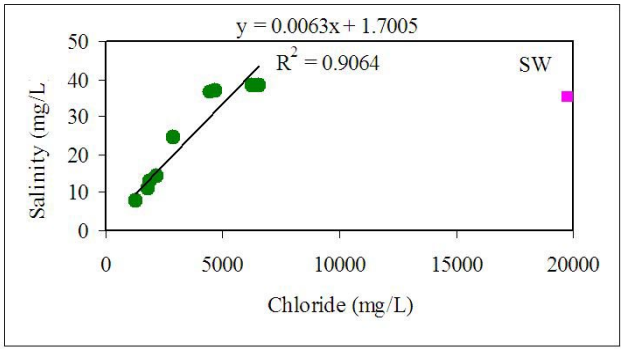

Figure 4. Variation of TDS vs. sampling points; sum of cations vs. sum of anions; salinity vs. chloride.

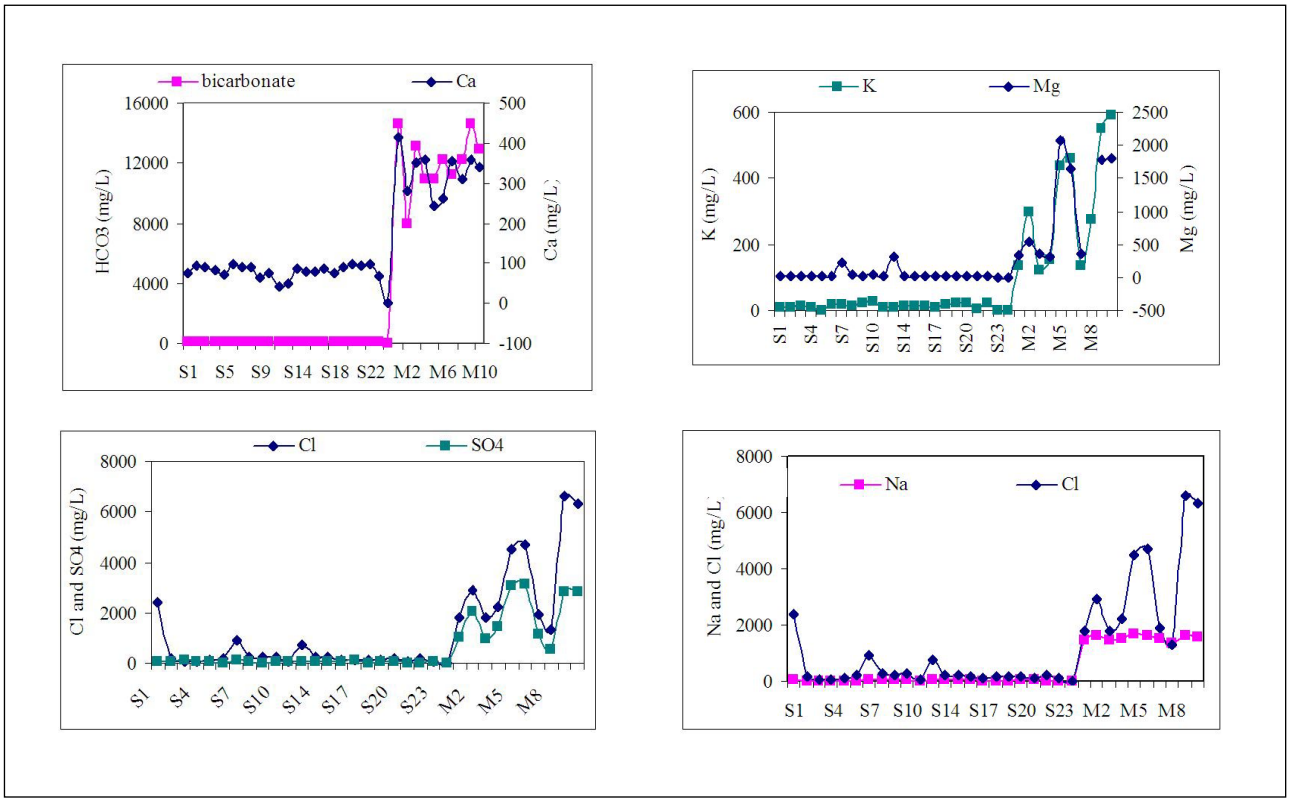

Figure 5. Spatial variation of some cations (mg/L) and anions (mg/L) for coastal and submarine studied sites.

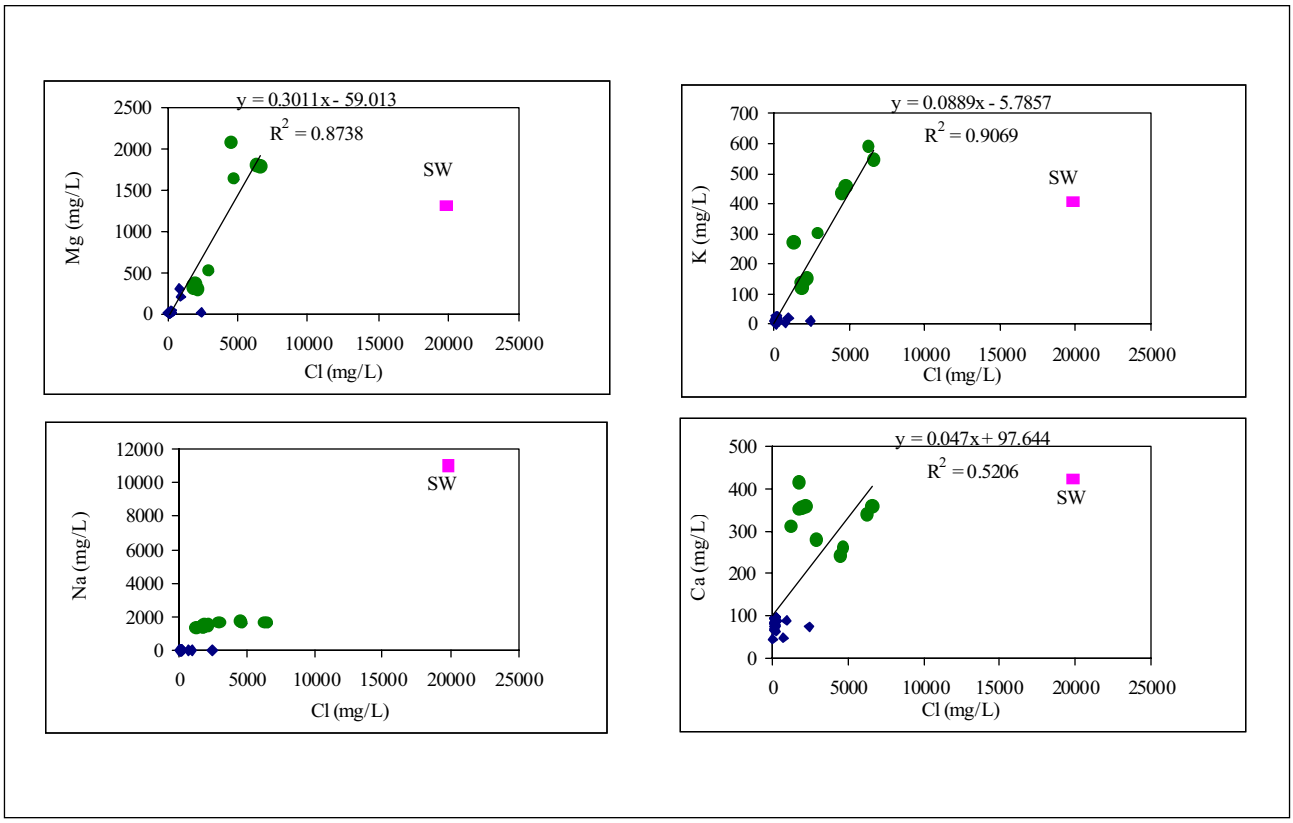

Figure 6. Plot of chlorine concentration vs. the concentrations of Mg, Na, K and Ca (mg/L) in coastal (♦) and submarine (●) springs.

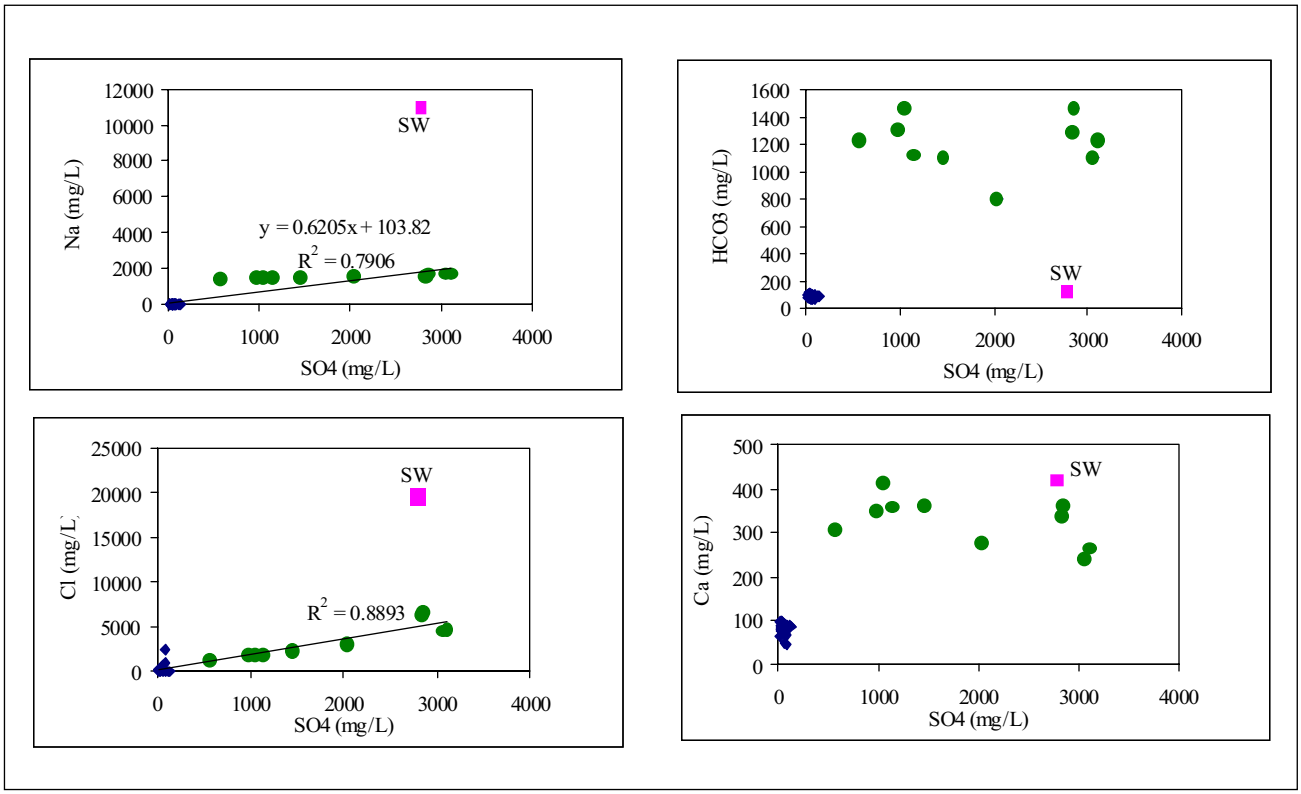

Figure 7. Plot of sulfate concentration vs. the concentrations of Na, Cl, HCO_3 and Ca (mg/L) in coastal (♦) and submarine (●) springs.

Sulfate results

Figure 7 shows a depletion of Na and Cl relative to seawater with a good correlation with the sulfate concentration. The depletion of these elements supports the previous explanation of seawater dilution. To account for a low Na and Cl content, a fresh water component is suggested compared to the composition of SW. These diagrams also show a high amount of sulfate in samples M5, M6, M9, M10, marking the distinct group in submarine samples defined earlier. A sulfate component input could explain these high values like the infiltration of contamination or the possibility of the existence of thermal sources, or even sources derived from confined or semi-confined aquifers. To settle this question, we need further analysis for environmental isotopes, especially for sulfur, to decide the origin of high concentrations of sulfate. Significant enrichment of HCO_3 and Ca are seen relative to SW. In this case interaction with the aquifer matrix could explain the presence of calcite minerals into the water (Tsunogai et al., 1996). In the case of magnesium, almost all waters are depleted relatively to seawater.

Isotopic analysis

The first seawater analysis for $\delta^{18}O$ was made by Epstein and Mayeda (1953). Based on their results, Craig (1961) defined Standard Mean Ocean Water. Large variations and deviations from $\delta^{18}O = 0‰$ and $\delta^{2}H = 0‰$ are found in seas and oceans, including Mediterranean sea water ($\delta^{18}O = +1.7‰$ and $\delta^{2}H = +10‰$). These variations can be due to evaporation (for example the equatorial surface water $\delta^{18}O = +0.7‰$), variable amounts of freshwater runoff in coastal waters from continental rivers, and variable amounts of meltwater in polar waters.

In the latter two cases $\delta^{18}O$ is linearly related to salinity, as in estuaries. In the first case evaporation

causes ^{18}O (deuterium) enrichment, which is therefore also correlated with salinity. The $\delta^{18}O/\delta^{2}H$ diagram (Figure 8) shows that coastal freshwaters are closer to the Mediterranean Meteoric Water Line (MMWL) than the submarine data. This indicates a rapid infiltration of meteoric water to recharge coastal aquifer groundwater. But all data are well correlated with a slope of 5.4 and a deuterium excess of +3.3‰. The difference with MMWL (defined with a slope of 8 and a deuterium excess of +22‰) indicates evaporative isotope enrichment, which is very pronounced in the submarine samples (Gat and Carmi, 1970).

Figure 8 also shows that coastal and submarine waters are correlated on the same line indicating the same hydrological origin for both. These waters come from the same aquifer in Cretaceous formations. Regarding plot 8, we can distinguish 3 groups of samples. Submarine M5, M6, M9 and M10 lie under the Global Meteoric Water Line (defined with a slope of 8 and a deuterium excess of +10‰) indicating a high mixing factor between coastal freshwater and seawater (excess ranges between 7 and –0.9‰). This confirms the physical and chemical results that separate them from other submarine samples. The special isotopic data (positive values) of this group is probably related to the type, nature and properties of water.

Samples (M1, M2, M3, M4, M7, M8) between MMWL and GMWL are characteristic of the common range for groundwater in the eastern Mediterranean region (Wagner and Geyh, 1999). They also exhibit an isotopic enrichment due to partial mixing of the freshwater and seawater indicated by relatively low deuterium excess values (excess ranges between 11 and 21‰). M8 falls within the coastal freshwater samples indicating a typical meteoric submarine spring. Coastal freshwater S5, S9, S10 and S11 are characterized by high excess (more than 22‰), and seem to reflect local meteoric water.

To get more information for different types of water, we have plotted the electrical conductivity of samples versus $\delta^{18}O$. In Figure 9 we see that coastal freshwaters reflect primarily coastal or mountain meteoric water recharge; Submarine springs show different mixing percentages with seawater and a very low mixing is observed in M8. End points in the diagram corresponding to M5, M6, M9, M10 have higher ECs than seawater, suggesting the possibility of thermal water or confined water or even contaminated water (high sulfate content).

On the basis of the above diagram, we used the following formula to calculate component-mixing parameter:

$$P(s) = (EC(s) - EC(\text{sample})) / (EC(s) - EC(f))$$

Where:

P(s)= proportion of seawater,

EC (s)= electrical conductivity of seawater,

EC (f)= electrical conductivity of coastal freshwater,

EC (sample)= electrical conductivity of corresponding submarine spring, and

P(f) = 1- P(s) where P(f) is the proportion of freshwater.

Results show the highest proportion of freshwater for the M8 sample. These percentages are plotted in Figure 10 versus$\delta^{18}O$, indicating a very high correlation between values. Thus the recharge origin of submarine water seems to be an admixture between freshwater from highly karstified

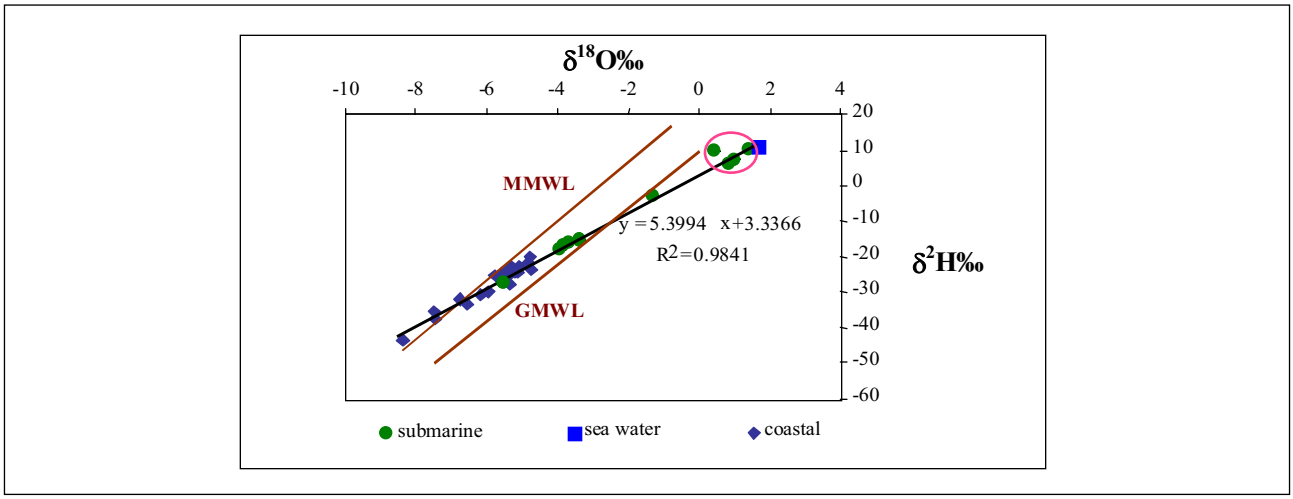

Figure 8. $\delta^{18}O/\delta^{2}H$ plot for coastal and submarine springs with the Mediterranean Meteoric Water Line (MMWL) and the Global Meteoric Water Line (GMWL).

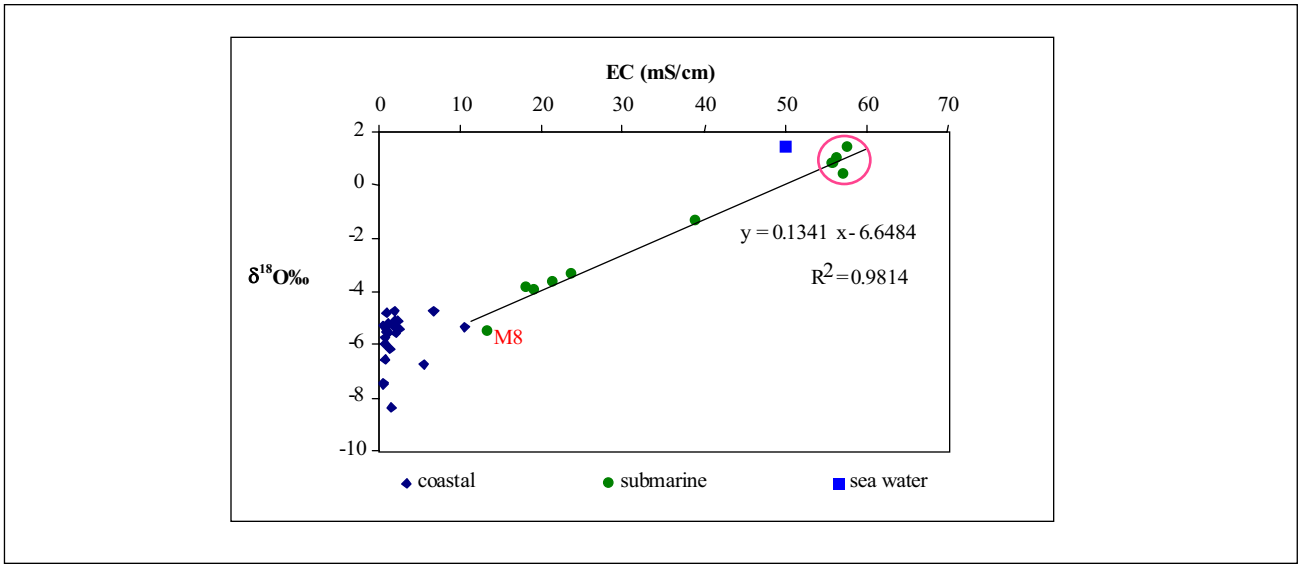

Figure 9. Relationship between $\delta^{18}O$ and electrical conductivity concentration of the coastal and submarine studied springs.

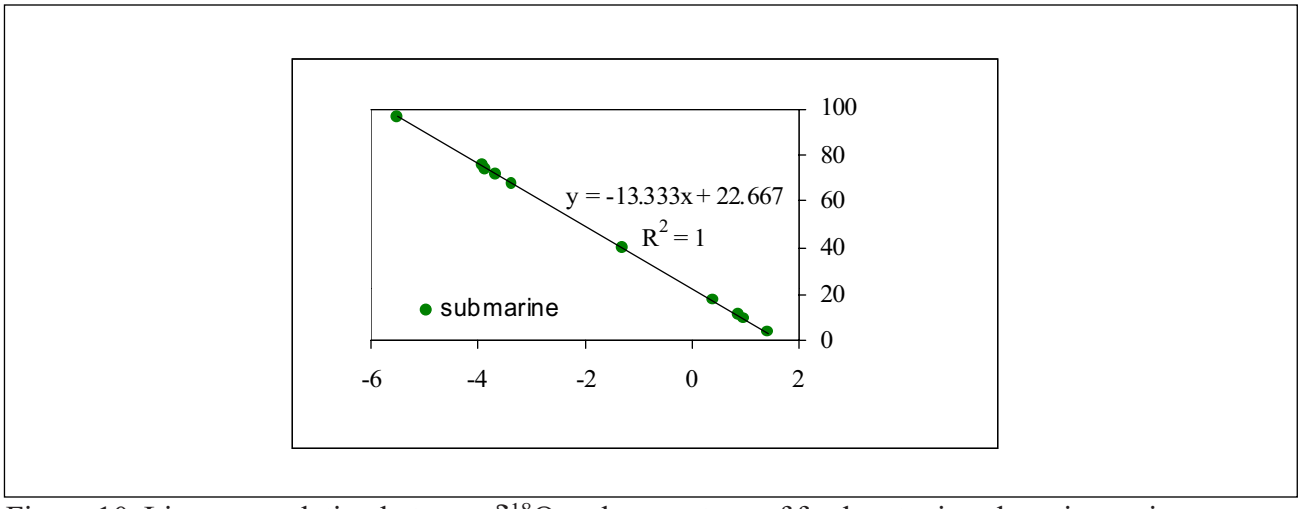

Figure 10. Linear correlation between $\delta^{18}O$ and percentage of freshwater in submarine springs.

aquifers in Cenomanian-Turonian formations (where meteoric water infiltrates easily) and seawater, especially in M5, M6, M9 and M10.

The previous formula used to calculate the component-mixing parameter is not very precise in some cases such as for the special group of M5, M6, M9, M10 submarine springs. To obtain more information from this group we plotted chlorine values versus $\delta^{18}O$ for submarine and coastal freshwater with the corresponding mixing line (Figure 11). The shape of the mixing line becomes horizontal for the special group of M5, M6, M9, M10 submarine springs. This group may contain water from thermal sources, confined aquifers or contamination sources (Geyh, 2000).

To date coastal and submarine freshwater, tritium values are plotted in Figure 12 versus $\delta^{18}O$. General tritium values range from 0.75 to 3.77 TU for submarine samples and range from 0.69 to 4.83 TU for coastal freshwater. In particular, we found similar values for ^{3}H in S6 (2.42 TU) and its corresponding submarine source M8 (2.95 TU). In Figure 12 we distinguish two major groups. The highest values show a mixing with young meteoric water, primarily in coastal water indicating constantly recharged water. The second group, containing the special M5, M6, M9, M10 correspond more likely to older water.

CONCLUSIONS

A combined hydrochemical and environmental isotope survey was conducted for 23 major freshwater coastal springs and 10 submarine springs. Preliminary hydrochemical results show different types of submarine and coastal springs consisting of two basic water types for submarine water and three basic water types for coastal water. The chemical facies for submarine water are Ca-Na-HCO_3-Cl and Ca-Mg-HCO_3-Cl in all samples. Whereas the facies for coastal sources are Ca-Mg-Cl, Ca-Mg-SO_4-Cl-HCO_3 and Ca-Mg-Cl-HCO_3. The sources are a Cenomanian -Turonian aquifer with a large influence of calcite and dolomite bedrock.

Physical and chemical analysis for submarine samples showed lower salinity, chloride, sodium, and potassium content. This was confirmed by sampling points derived essentially from freshwater sources in the marine field. Almost all waters are enriched in Ca and Mg relative to the seawater dilution line. This implies that dissolution of Ca and Mg minerals such as calcite and dolomite has occurred. Possible sources of these elements are the Upper Cretaceous and Eocene carbonate rocks that are found throughout much of the region. All physical and chemical analysis show different characteristics for the M5, M6, M9, M10 group of submarine springs, especially an excess of sulfate. Possible sources of sulfate are thermal water, confined aquifers or infiltration of contamination.

Isotopic data for $\delta^{18}O/\delta^{2}H$ showed that coastal freshwaters are closer to the Mediterranean Meteoric Water Line (MMWL) than the submarine data. Submarine M5, M6, M9 and M10 lie under the Global Meteoric Water Line (defined with a slope of 8 and a deuterium excess of +10‰) indicating a high mixing factor between coastal freshwater and seawater (deuterium excess range between 7 and –0.9‰). Isotopic results also confirmed the presence of different aquifer characteristics (confined, semi-confined or thermal water) for these submarine samples that influence the water quality. Samples M1, M2, M3, M4, M7, M8 between MMWL and GMWL are characteristic of the common range for groundwater in the eastern Mediterranean region. M8 is characterized by at least 96% freshwater. Coastal freshwaters S5, S9, S10 and S11 are characterized by high deuterium excess (more than 22‰), and seem to reflect local meteoric water.

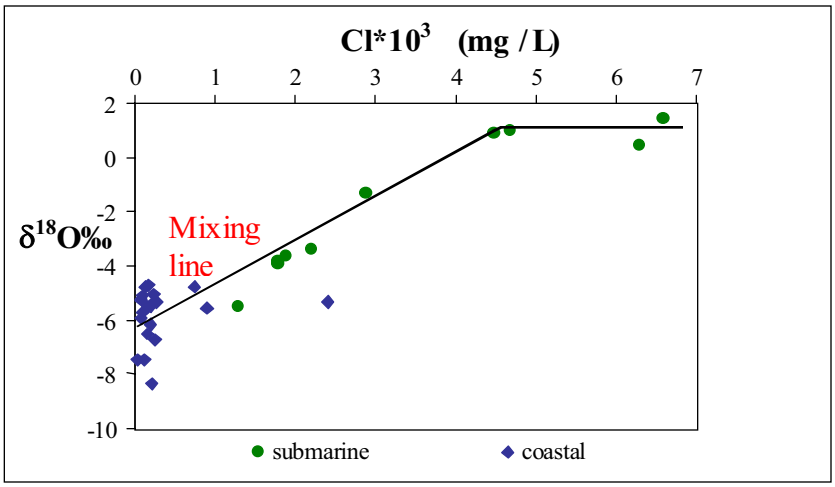

Figure 11. Relationship between $\delta^{18}O$ and chlorine concentration of the coastal and submarine springs.

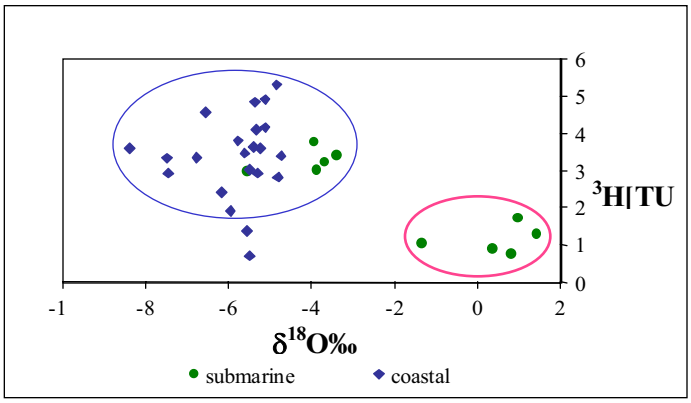

Figure 12. Variation of tritium values versus $\delta^{18}O$ for all coastal and submarine springs.

ACKNOWLEDGMENTS

The authors gratefully acknowledge the support of the Lebanese – Syrian scientific cooperation program.

REFERENCES

Astraldi, M., and G.P. Gasparini. 1992. The seasonal characteristics of the circulation in the north Mediterranean basin and their relationship with the atmospheric-climatic conditions. Journal Geophysical Research, 97: 9531-9540.

Béthoux, J.P., and B. Gentili. 1996. The Mediterranean sea: coastal and deep sea signatures of climatic and environmental changes. Journal of Marine Systems, 7: 383-394.

Béthoux, J.P., and B. Gentili. 1999. Functioning of the Mediterranean sea: past and present changes related to freshwater input and climate changes. Journal of Marine Systems, 20: 33-47.

Beydoun, Z. R. 1977. The Levantine countries: the geology of Syria and Lebanon (maritime regins), In: Nairn, A. E. M., Kanes, W. H. and Stehli, F. G., (Eds)., The Ocean Basins And Margins: volume 4A; The Eastern

Mediterranean, New York, Plenum Press, 319-353.

Bryden, H.L., J. Candela, and T.H. Kinder. 1994. Exchange through the strait of Gibraltar. Progress in Oceanography, 33: 201-248.

Craig, H. 1961. Standards for reporting concentrations of Deuterium and oxygen-18 in natural waters. Science, 133: 1833-1834.

Dubertret, L. 1966. Liban, Syrie et bordure des pays voisins. Première partie. Tableau stratigraphique avec carte géologique au millionième. Notes et Mém. Moyen Orient, 8, 251-358.

Dubertret, L. 1975. Introduction à la carte géologique à 1/50000 du Liban. Notes et Mém. Moyen-Orient, 23, 345-403.

Epstein, S., and T. Mayeda. 1953. Variation of oxygen-18 content of waters from natural sources. Geochimica Cosmochimica Acta, 4: 213-224.

FAO. 1972. Projet de développement hydro-agricole du Liban. Thermometrie aéroportée par infrarouge.

Gat, J.R., and I. Carmi. (1970) Evolution of the isotopic composition of atmospheric water in the Mediterranean sea area.– J. Geophys. Res., 75 (15), 3039-3048.

Geyh, M.A. 2000. An overview of ^{14}C analysis in the study of groundwater. Radiocarbon, vol. 42, no. 1, pp. 99-114.

Gruvel, A. 1931. Les états de Syrie. Richesses marines et fluviatiles. Exploitation actuelle, Avenir. Paris.

Guerre, A. 1969. Etude comparative du tarissement des principales sources karstiques du Liban. PhD thesis, Montpellier, france.

Hakim, B. 1976. Détection des sources sous-marines et littorales du Liban par thermoradiométrie infra-rouge. Méditérranée, 4:31-38.

Hakim, B. 1985. Recherches hydrologiques et hydrochimiques sur quelques karsts méditérranéens Liban, Syrie et maroc. Publications de l'Université Libanaise, 701pp.

Hecht, A., N. Pinardi , and A. Robinson. 1988. Currents, water masses, eddies and jets in the Mediterranean Levantine basin. Journal Physical Oceanography,18:1320-1353.

Khawlie, M., A. Shaban, and C. Abdallah. 2000. Evaluating the potentials of submarine springs: an unconventional water source for the coastal area – Lebanon. ESCWA, Expert group meeting, Beirut.

Krahman, E.J., and H.L. Schott. 1998. Longterm increases in the western Mediterranean salinities and temperatures: anthropogenic and climatic sources. Geophysical Research letters, 22: 4209-4212.

MEDATLAS Group. 1997. A Mediterranean hydrographic Atlas from a composite quality checked temperature and salinity data, IFREMER (ed.)

Mijatovic, B., and M. Bakic. 1967. le karst du Liban, etude de son evolution d'après les recherches hydrogéologiques. BRGM, Chronique d'hydrogéologie, Paris, 10: 95-107.

NCRS. 1997. Preliminary report on project of TIR survey along the coast of Lebanon.

Qareh, R.1966. The submarine springs of Chekka, exploitation of a confined aquifer discharging in the sea. PhD thesis, geology department, American University of Beyrouth.

Saad, Z., V.A. Kazpard , M.A.Geyh, and K. Slim. 2004. Chemical and Isotopic Compositions of Water from Springs and Wells in the Damour River Basin and the Coastal Plain in Lebanon. Journal of Environmental Hydrology, 12:1-13.

Shaban, A., M. Khawlie, and C. Abdallah. 2001. New water resources for southern Lebanon: thermal Infra-red remote sensing of submarine springs. Conference AUB, National center for Remote Sensing-NCRS.

Sturchio, N.C., G.B. Arehart, M. Sultan, Y. Sano, Y. AboKamar, and M. Sayed. 1996. Composition and origin of thermal waters in the Gulf of Suez area, Egypt. Applied geochemistry, 11: 471-479.

Tsunogai, U., J. Ishibashi, H. Wakita , T. Gamo , T. Masuzawa , T. Nakatsuka , Y. Nojiri, and T. Nakamura. 1996. Fresh water seepage and pore water recycling on seafloor: sagami through subduction zone, Japan. Earth and planetary Science letters, 138: 157-168.

Vengosh, A., C. Helvaci, and I.H. Karamanderesi . 2002. Geochemical constraints for the origin of thermal waters from western Turkey. Applied Geochemistry, 17: 163-183.

Walley, C. D. 1988. A braided strike-slip model for the northern continuation of the Dead Sea Fault and its implications for Levantine tectonics. Tectonophysics,145, 63-72.

Walley, C. D. 1998. The lithostratigraphy of Lebanon: A review Lebanese Science Bulletin 10, (1) 81-108.

Wagner, W., and M.A. Geyh. 1999. Application of environmental isotope methods for groundwater studies in the ESCWA region.– ESCWA/IAEA, 53 pp.; Beirut.

ADDRESS FOR CORRESPONDENCE
Zeinab Saad
Lebanese Atomic Energy Commission
CNRS, P.O.Box 11-8281
Riad El-Solh 1107 2260
Beirut, Lebanon

Email: z.saad@cnrs.edu.lb